Characterization and Comparison of High Blocking Voltage IGBTs and IEGTs under Hard- and Soft-Switching Conditions

Kansuke Fujii, Peter Koellensperger and Rik W. De Doncker
RWTH Aachen University
Institute for Power Electronics and Electrical Drives
D-52066, Aachen, Germany
Email: fj@ieee.org

Abstract— **The market continues to require IGBTs with higher blocking voltages to reduce the number of IGBTs connected in series in high voltage converters. To cope with these demands, semiconductor manufactures have developed several technologies. Nowadays, IGBTs up to 6.5 kV blocking voltage and IEGTs up to 4.5 kV blocking voltage are on the market. However, these IGBTs and IEGTs still have very high switching losses compared to low voltage devices, leading to a realistic switching frequency of up to 1 kHz. To reduce switching losses in high power applications, the Auxiliary Resonant Commutated Pole Inverter (ARCPI) is a possible alternative. In this paper, switching losses and on-state voltages of NPT-IGBT (3.3 kV-1200 A), FS-IGBT (6.5 kV-600 A), SPT-IGBT (2.5 kV-1200 A, 3.3 kV-1200 A and 6.5 kV-600 A) and IEGT (3.3 kV-1200 A) are measured under hard-switching and zero-voltage switching (ZVS) conditions. The aim of this selection is to evaluate the impact of ZVS on various devices of the same voltage ranges. In addition, the difference in ZVS effects among the devices with various blocking voltage levels is evaluated.**

I. Introduction

The market needs IGBTs with high blocking voltages and small switching losses. However, these performances have a trade-off relation. To improve this trade-off, semiconductor companies have developed several technologies. There are Field Stop (FS), Soft Punch Through (SPT) technology and Injection Enhanced Gate Transistor (IEGT) technology. Such technologies make it possible to achieve nearly the silicon semiconductor limit. Nowadays, the FS technology is applied to 6.5 kV-IGBTs[1], [2], [3], as well as the SPT technology[4], [5]. In addition, IEGTs with blocking voltages up to 4.5 kV are available[6], [7], [8]. However, all these IGBTs and IEGTs still have very high switching losses, thus, in practice, the switching frequency is limited to about 1 kHz. If such devices are used in inverters connected to transmission lines (e.g. STATCOMs), high switching frequencies are necessary to achieve low harmonic distortion of the current without large filters.

To reduce switching losses, soft-switching technologies are widely known. Especially, Auxiliary Resonant Commutated Pole Inverters (ARCPI)[9], [10] are desirable in high power applications[11], because required voltage and current rating of the switching devices in the ARCPI are nearly the same as these of the devices in hard-switched inverters. Several authors have already compared switching losses of specific high blocking voltage devices in hard-switched inverters and ARCPIs[11], [12]. In [11], the behavior of IGCTs (4.5 kV) at hard- and soft-switching is described, and IGCTs in ARCPIs are compared with IGCTs in conventional snubberless topologies. Furthermore, in [12], the PT and NPT IGBTs (1.2 kV) with trench-gate are mainly compared with standard IGBTs in zero-voltage and zero-current switching operation.

At present, almost all topologies used are conventional hard-switching inverters. Thus, device manufactures produce IGBTs, which are optimized for hard-switching operation. Even if the numbers of ARCPI would be increased, the IGBTs for hard-switching topologies would be applied, because non-standard devices remain very expensive. Therefore, it is necessary to choose optimal devices for the ARCPI among commercial devices, which are produced for hard-switching inverters.

In this paper, five different IGBTs (from 2.5 kV to 6.5 kV blocking voltage) and 3.3 kV IEGT are evaluated at several voltages, currents and temperatures. To measure such many cases effectively, an automatic measurement system controlled by a PC with LabVIEW has been developed. In the measurements, switching energies under hard- and soft-switching conditions are evaluated, and ZVS effects on the basis of auxiliary capacitors are presented.

II. Evaluated Devices

When device engineers design a device, they have two basic choices. There are punch-through (PT) and non-punch-through (NPT) devices. NPT can be fabricated at low cost, but produce high switching losses because of the thick n-drift region. On the other hand, PT needs starting material with very high resistivity to achieve high blocking voltage with low cosmic ray failure probability. Thus, PT is not desirable for high blocking voltage devices. Therefore, several manufactures have developed technologies, which are located between PT and NPT. In this paper, such devices, shown in Table I, are evaluated under hard- and soft-switching conditions.

Manufacture A has developed the Field-Stop (FS)-technology and applied it to IGBTs with a blocking voltage of 6.5 kV. FS-technology is based on NPT technology. The Field Stop Zone is injected on the shallow p-emitter as shown

Authorized licensed use limited to: Infineon Technologies AG. Downloaded on January 16,2023 at 08:48:59 UTC from IEEE Xplore. Restrictions apply.

in Fig. 1(a). The 3.3 kV IGBT evaluated in this paper is not yet a FS-IGBT. This IGBT will be fabricated with the FS-technology in the near future, but the FS-technology is now applied to 6.5 kV and up to 1.7 kV IGBTs[13].

Manufacture B has developed the Soft-Punch-Through (SPT)-technology and applied it to IGBTs with blocking voltage up to 6.5 kV. SPT-technology basically consists of a low doped n-base and SPT n-buffer as shown in Fig. 1(b), and makes the switching behavior of normal PT devices more softly. In other words, di/dt during switching (especially turn-off) becomes lower than that of a PT device.

Manufacture C has developed the IEGT-technology to replace GTOs with IEGTs. To achieve a low on-state voltage like a thyristor, the IEGT is designed so that many electrons accumulate at the electrodes as shown in Fig. 1(c). The IEGT-technology is now applied to 4.5 kV press-pack devices and 3.3 kV module devices.

In this paper, six devices shown in Table I and diodes in the same packages are evaluated. The reason of this selection is to evaluate difference of the ZVS effect in the various devices of the same voltage ranges. In addition, difference of the ZVS effect among the various blocking voltage should be evaluated.

TABLE I
EVALUATED DEVICES

Manufacturer	Device	V_{CES}(V)	I_C(A)
A	NPT-IGBT	3300	1200
	FS-IGBT	6500	600
B	SPT-IGBT	2500	1200
		3300	1200
		6500	600
C	IEGT	3300	1200

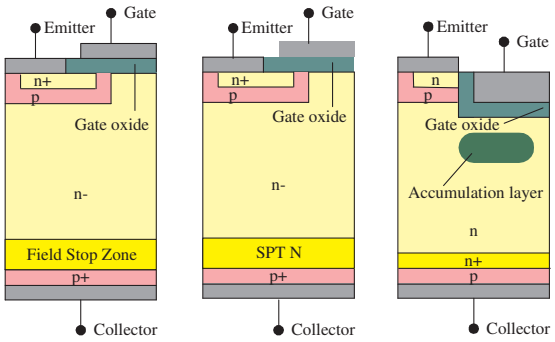

(a) FS-IGBT (b) SPT-IGBT (c) IEGT

Fig. 1. Device structure

III. A TEST BENCH FOR HIGH BLOCKING VOLTAGE DEVICES

A. Automatic measurement system

To calculate actual operational losses, i.e. switching losses and conduction losses at different operating condition, measurements of switching energy and on-state voltage at several currents, several dc-link voltages and several junction temperatures are necessary. For any one device to be evaluated, more than one hundred double pulse tests must be done. To execute many cases properly, an automatic measurement system becomes necessary. The automatic measurement system is shown in Fig. 2. This system consists of a PC with LabVIEW, an optical converter, a PC oscilloscope, a pulse generator for soft-switching operation and a test bench. LabVIEW supplied by National Instruments is useful to configure sequential control systems with a graphic user interface. The PC and the high voltage area surrounded with the dashed line in Fig. 2 are isolated by using optical signals, and the high voltage area is enclosed with a cage connected to the ground.

In this system, the PC generates three pulses to execute the double pulse test and a trigger for the PC oscilloscope. In addition, the PC gathers measurement data, which is acquired with the PC oscilloscope. The interface between the PC and the oscilloscope is realized with an optical USB. To judge whether the test condition is ready or not ready, the dc-link voltage (E_{dc}) and the junction temperature (T_j) are measured and sent to the PC directly. Actually, it is impossible to measure T_j directly. Therefore, the case temperature is measured as T_j after thermal equilibrium. In order to send such analog signals to the PC with optical signals, these signals are modulated at high frequency. Thus, pulses at high frequency based on the actual values of E_{dc} and T_j are changed to optical signals and sent to the optical converter.

In this measurement, two gate drivers are used. One of them is a gate driver used to measure 6.5 kV-IGBT[14], and the other, which is optimized for hard-switched 3.3 kV-NPT-IGBT, is used to measure 3.3 kV- and 2.5 kV-IGBT. Thus, devices with the same blocking voltage are evaluated by using the same gate driver.

Usually, a step-down chopper circuit is used to evaluate switching energy measurement. In this circuit, large capacitors are necessary to keep the DC-link voltage constant, when the test current is very high. For this reason, a step-up chopper circuit using two separate dc-links, shown in Fig. 3, is used to characterize the devices. In this test bench, the low voltage capacitor (C_{LV}) supplies currents to the Device Under Test (S_{DUT}), and the energy stored in the inductance (L_1) is transferred to the high voltage capacitors (C_{HV1} and C_{HV2}). In addition, the current does not increase during the second turn-on period.

B. Switching energy measurement of soft-switched devices

If the switching energy under ZVS conditions is measured, auxiliary capacitors (C_{r1} and C_{r2}: from 0.5 μF to 3 μF) are connected parallel to the S_{DUT} and D_{DUT} as shown in Fig. 3. Furthermore, auxiliary switches (S_{RES} and D_{RES}) and an auxiliary inductance (L_{aux}: 4.4 μH) are connected between the inductance (L_1) and the neutral point of the high voltage capacitors (C_{HV1} and C_{HV2}). The reason C_{HV2} is larger than C_{HV1} is that the boost current [10] to compensate the loss of the resonant circuit is not applied in this test bench.

The command of S_{RES} is generated with the Auxiliary signal generator shown in Fig. 2. The generator receives the

Authorized licensed use limited to: Infineon Technologies AG. Downloaded on January 16,2023 at 08:48:59 UTC from IEEE Xplore. Restrictions apply.

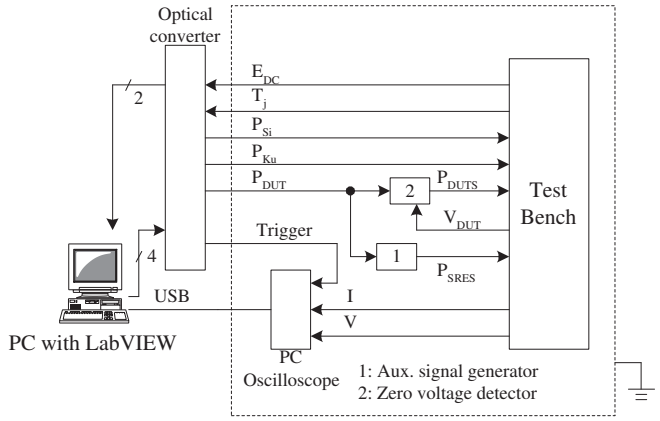

Fig. 2. Configuration of the high voltage devices evaluation system

pulse of the S_{DUT} (P_{DUT}) and generates a pulse, whose width is longer than the commutation time of the auxiliary capacitors, in order to turn off the S_{RES} with zero current. The P_{DUT} sent by the PC does not take into account the zero-voltage switching. The zero-voltage detector shown in Fig. 2 observes the voltage of the S_{DUT} (V_{DUT}) and sends the on-command to the gate driver, if the voltage is below the zero-voltage level (about 200V).

In the soft-switching measurement, only the turn-off energy is measured, because the turn-on energy of the ARCPI is ideally negligible; and besides, it is very difficult to evaluate a low collector-emitter voltage of the S_{DUT} during turn-on with a high-voltage probe.

The behavior of this test bench is as shown in Fig. 4.

1) $t_0 \leq t < t_1$*:* Initially, V_{DUT} is equal to the voltage of the PS_H, because the collector of S_{DUT} is connected to PS_H with the resistor R_{ini}. Then, both S_i and S_{RES} are turned on, and commutation of S_{DUT} starts. The resonant current flows through C_{r1}, C_{r2}, L_{aux}, S_{RES}, D_{RES}, C_{HV1} and C_{HV2}.

2) $t_1 \leq t < t_2$*:* When V_{DUT} becomes zero, S_{DUT} is turned on. This forces the current of the inductance (I_L) to increase up to the test current. I_L flows through C_{LV}, S_i, D_{blc}, L_1 and S_{DUT}.

3) $t_2 \leq t < t_3$*:* S_{DUT} is turned off and the current of S_{DUT} is commutated to the auxiliary capacitors. I_L flows through C_{LV}, S_i, D_{blc}, L_1, C_{r1}, C_{r2}, C_{HV1} and C_{HV2}.

4) $t_3 \leq t < t_4$*:* V_{DUT} becomes the DC-link voltage, and I_L is commutated to D_{DUT}. To keep I_L constant, S_{ku} is turned on. By turning on S_{ku}, the current through S_i is reduced to zero, and S_i is turned off with zero current. To achieve this, P_{Si} is kept high after t_3. I_L flows through L_1, D_{DUT} and S_{ku}.

5) $t_4 \leq t < t_5$*:* S_{ku} is turned off to start the measurement of the switching energy. I_L flows through D_{fw}, D_{blc}, L_1, D_{DUT}, C_{HV1} and C_{HV2}.

6) $t_5 \leq t < t_6$*:* At t_5, S_{RES} is turned on, and the commutation from D_{DUT} to S_{DUT} starts. At this moment, the reverse-recovery energy of D_{DUT} is measured. I_L flows through D_{fw}, D_{blc} and L_1. A part of I_L flows through D_{DUT}, C_{HV1} and C_{HV2}, and the other flows through L_{aux}, S_{RES}, D_{RES} and C_{HV2}.

7) $t_6 \leq t < t_7$*:* The current of D_{DUT} becomes zero, and the resonance between the auxiliary capacitors and L_{aux} starts. V_{DUT} is reduced to zero by this commutation. I_L flows through D_{fw}, D_{blc} and L_1, C_{r1}, C_{r2}, L_{aux}, S_{RES}, D_{RES}, C_{HV1} and C_{HV2}.

8) $t_7 \leq t < t_8$*:* When V_{DUT} becomes zero, S_{DUT} is turned on. I_L flows through D_{fw}, D_{blc}, L_1 and S_{DUT}.

9) $t_8 \leq t$*:* Finally, S_{DUT} is turned off, and the turn-off energy is measured. I_L is commutated to the auxiliary capacitors, and then the energy of L_1 is transferred to C_{HV1} and C_{HV2} through D_{DUT}. I_L flows through D_{fw}, D_{blc}, L_1, D_{DUT}, C_{HV1} and C_{HV2} after commutation.

If the device is measured under hard-switching conditions, R_{ini}, C_{r1}, C_{r2}, L_{aux}, S_{RES} and D_{RES} are removed, and S_{DUT} is switched on and off by using P_{DUT}.

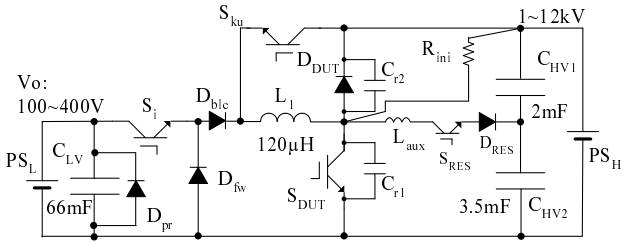

Fig. 3. Circuit of the soft-switching test bench

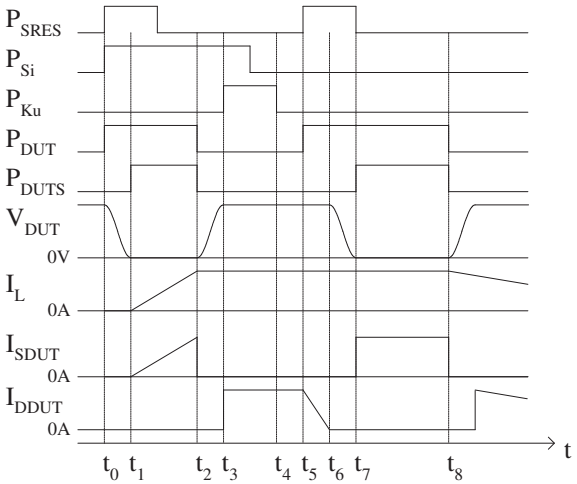

Fig. 4. Double Pulse and current during soft-switching measurements

IV. Measurement Results and Discussions

A. Hard-switching energy versus current

The test bench has been programmed to carry out automatically 120 different cases for each device under a certain switching condition (6 junction temperatures×4 voltage levels×5 current levels). One of the results is shown in Fig. 5. From this waveform, the turn-on energy and the turn-off energy of the devices are calculated. In addition, the test current and the voltage are also measured. In the PC with LabView, the current before the turn-off command is assumed

Authorized licensed use limited to: Infineon Technologies AG. Downloaded on January 16,2023 at 08:48:59 UTC from IEEE Xplore. Restrictions apply.

as the test current, and the voltage before the turn-on command is recorded as the test voltage.

After 20 tests, turn-on and -off energies at 120°C as shown in Fig. 6 and Fig. 7 are obtained automatically. To compare the results under hard- and soft-switching conditions, the switching losses measured under certain temperature, voltage and current levels are necessary. However, it is difficult to achieve these measurements under equal test voltage and current level, because the delay time of S_{ku} changes on the basis of the test voltage and the test current. Thus, interpolating functions are derived from the measurement results to compare switching losses at the nominal current and voltage. The functions are shown in (1) to (3).

$$f(x) = a_2 x^2 + a_1 x + a_0 \tag{1}$$

$$E_{OFF} = f(I_c),\ a_n = f(V_{ce}),\ n = 0, 1, 2 \tag{2}$$

$$E_{ON} = f(I_c),\ a_n = f(V_{ce}),\ n = 0, 1, 2 \tag{3}$$

The turn-off and turn-on energies under hard-switching are interpolated by using the quadratic function of the test currents. In addition, the coefficients (a_2, a_1 and a_0) are also interpolated by the quadratic function of the test voltages. The error caused by this interpolation is less than 0.1%.

To measure the reverse-recovery energies, the position of the current sensor and voltage sensor is changed. One of the measurement waveforms is shown in Fig. 8. The PC with LabView takes the current before the turn-on command of the switch as the test current, and the voltage before the turn-off command of the switch is recorded as the test voltage. In addition, the reverse-recovery energy is obtained by integrating $I_f \times V_{AK}$. After 20 chopper tests, the reverse-recovery energies at 120°C as shown in Fig. 9 are obtained automatically. In order to compare these energies with the energies of the soft-switched diode, they are modeled in the same manner with the turn-on and -off energies. The energies are interpolated by using (4). $f()$ is defined by (1).

$$E_{rr} = f(I_f),\ a_n = f(V_{AK}),\ n = 0, 1, 2 \tag{4}$$

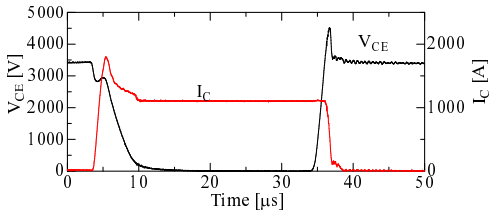

Fig. 5. Waveforms of the 6.5 kV SPT-IGBT under hard-switching condition

B. Soft-switching energy versus current

During the measurement of the soft-switching conditions, the turn-off energy is evaluated for the reason shown in section III-B. One of the waveforms obtained in the measurement is shown in Fig. 10. The PC with LabView samples the

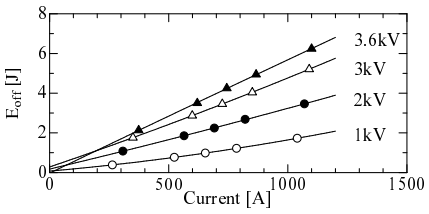

Fig. 6. Turn-off energy vs. current of 6.5 kV SPT-IGBT under hard-switching condition at 120°C

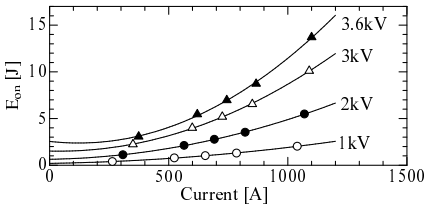

Fig. 7. Turn-on energy vs. current of 6.5 kV SPT-IGBT under hard-switching condition at 120°C

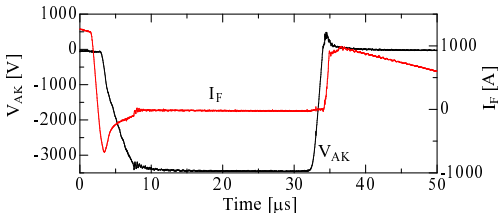

Fig. 8. Waveforms of the diode with 6.5kV-SPT-IGBT under hard-switching condition

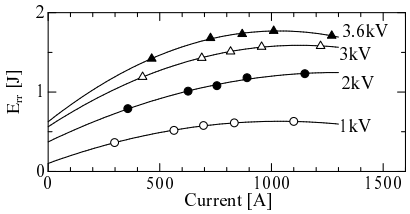

Fig. 9. Reverse-recovery energy vs. current of the diode with the 6.5kV SPT-IGBT under hard-switching condition at 120°C

current before the turn-off command as the test current, and the voltage at 50 μs is recorded as the test voltage. After 20 tests, turn-off energies at 120°C as shown in Fig. 11 are obtained automatically. From these results, it is clear that turn-off energies are saturated, even if the test voltage (V_{CE}) is increased. It is known that the turn-off energy under soft-switching condition is related to the tail current of the switch. The tail current disappears almost 10 μs after the turn-off command. Thus, the turn-off energy is not changed, even if V_{CE} is increased after the tail time.

The turn-off energies are interpolated by (5) and (6), in order to compare them with the energies under hard-switching condition. The equation to interpolate the energies by the current is the first-order function. In addition, the coefficients (a_1 and a_0) are interpolated by the quadratic function of the test voltages. $f()$ is defined by (1). The error caused by this

Authorized licensed use limited to: Infineon Technologies AG. Downloaded on January 16,2023 at 08:48:59 UTC from IEEE Xplore. Restrictions apply.

interpolation is less than 0.1%.

$$g(x) = a_1 x + a_0 \tag{5}$$

$$E_{OFF} = g(I_c),\ a_n = f(V_{ce}),\ n = 0, 1 \tag{6}$$

Furthermore, reverse-recovery energies of the soft-switched diodes are measured as shown in Fig. 12 and interpolated by the same manner with the turn-off energies under soft-switching condition as shown in (7). $f()$ is defined by (1).

$$E_{rr} = g(I_f),\ a_n = f(V_{AK}),\ n = 0, 1 \tag{7}$$

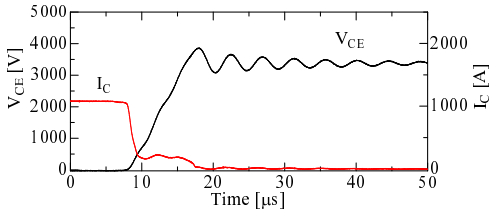

Fig. 10. Waveforms of the 6.5kV SPT-IGBT under soft-switching condition (C_{r1}, C_{r2} = 1 μF)

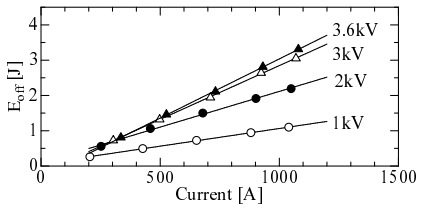

Fig. 11. Turn-off energy vs. current of 6.5kV SPT-IGBT under soft-switching condition at 120°C (C_{r1}, C_{r2} = 1 μF)

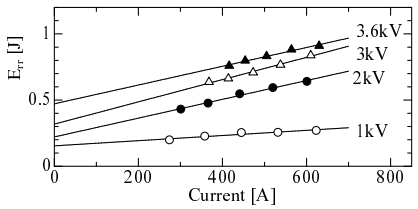

Fig. 12. Reverse-recovery energy vs. current of the diode with the 6.5kV SPT-IGBT under soft-switching condition at 120°C (C_{r1}, C_{r2} = 1 μF)

C. Auxiliary capacitors versus turn-off energy

In this section, the turn-off energies at nominal current, voltage and 120 °C are compared among the evaluated devices. The effect on the turn-off energy from ZVS in ARCPI depends on the size of the auxiliary capacitor. In this paper, several auxiliary capacitors are used to change the effect on the turn-off energy.

Fig. 13 shows the turn-off energies and reduction rates of the IGBTs with the blocking voltage of 6.5 kV. The reduction rate (RR) is calculated with (8).

$$RR[\%] = (1 - E_{OFF_{SS}}/E_{OFF_{HS}}) \times 100 \tag{8}$$

$E_{OFF_{SS}}$ is an energy of the soft-switched devices, and $E_{OFF_{HS}}$ is an energy of the hard-switched devices. During the measurement of the 6.5 kV-IGBTs, using auxiliary capacitor more than 1 μF leads to long commutation time at the small test current. Thus, only 0.5 μF and 1 μF are used. The results show that the ZVS effects on the SPT-IGBTs and FS-IGBTs with 6.5 kV blocking voltage are very similar to each other, and the reduction rate of 50 % is achieved by connecting 1 μF to the switch. Fig. 16 shows the trade-off relation (On-state voltage (V_{ON}) vs. Turn-off energy (E_{ON})) during device design. Two points enclosed with a circle with 6.5 kV are evaluated at nominal condition. V_{ON} is measured at 600 A and 120 °C, and E_{ON} is measured at 600 A, 3.6 kV and 120 °C. The devices with similar reduction rate are designed at the same trade-off point.

Fig. 14 shows the turn-off energies and reduction rates of the IGBT with the blocking voltage of 3.3 kV. To measure the 3.3 kV-IGBTs and IEGT, auxiliary capacitors (from 0.5 μF to 3 μF) are connected to the switch (S_{DUT}) and the diode (D_{DUT}). The results show that the reduction rate of the IEGT is smaller than that of other IGBTs (SPT-IGBT and NPT-IGBT), if the auxiliary capacitors are small. The IEGT has the accumulation layer of electrons in the n-base to decrease the on-state voltage. This results in long tail current time, which deteriorates the ZVS effect. The difference of the trade-off relation shown in Fig. 16 is very clear. This V_{ON} is measured at 1200 A and 120 °C, and E_{OFF} is measured at 1200 A, 1.8 kV and 120 °C. The IEGT has small on-state voltage and high E_{OFF}. One can say that this IEGT is designed for converters with low switching frequency like GTO converters. Even if the reduction rate is different at the measurements with small auxiliary capacitor, it becomes similar at the measurements with 3 μF. The fact, that the tail current time is limited, leads to a reduction rate for different devices, which becomes equal, when measurements are done with large auxiliary capacitors.

Fig. 15 shows the turn-off energies and reduction rates of the IGBT with a blocking voltage of 2.5 kV. In this measurement, auxiliary capacitors (from 0.5 μF to 3 μF) are connected to the switch (S_{DUT}) and the diode (D_{DUT}). The result of the reduction rate is very similar to the result of the SPT-IGBT with 3.3 kV blocking voltage.

If the reduction rate of different blocking voltage devices is compared, the reduction rate of 6.5 kV IGBTs is higher than that of other switches. It means that ZVS has a stronger impact on high voltage devices than that on devices with lower blocking voltage.

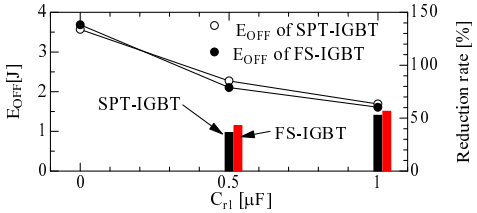

Fig. 13. Turn-off energy of 6.5 kV IGBT at 3600 V, 600 A and 120 °C

Authorized licensed use limited to: Infineon Technologies AG. Downloaded on January 16,2023 at 08:48:59 UTC from IEEE Xplore. Restrictions apply.

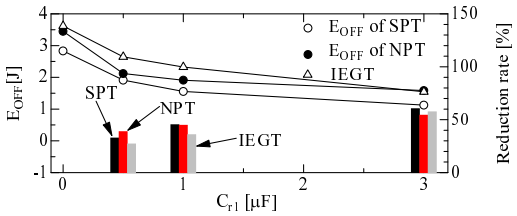

Fig. 14. Turn-off energy of 3.3 kV devices at 1800 V, 1200 A and 120 °C

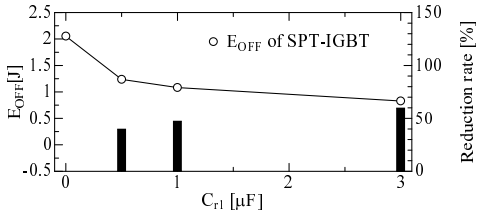

Fig. 15. Turn-off energy of 2.5 kV device at 1250 V, 1200 A and 120 °C

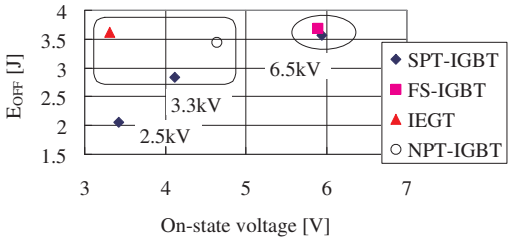

Fig. 16. On-state voltage and turn-off energy of IGBTs at nominal voltage, current and 120°C

D. Auxiliary capacitors versus reverse-recovery energy

Here, the reverse-recovery energies of the D_{DUT} are compared as well as S_{DUT}. The reverse-recovery energy in ARCPI depends on the di/dt during falling current and voltage changing during reverse recovery. In this paper, several auxiliary capacitors, which influence the reverse-recovery voltage, are used.

Fig. 17 shows the reverse-recovery energies and reduction rates of the diodes with the blocking voltage of 6.5 kV. The reduction rate of the reverse-recovery energies of the diode with the FS-IGBT (FS-diode) is quite different from that of the diode with the SPT-IGBT (SPT-diode). Though the reverse-recovery energy of the SPT-diode is reduced to 60 % of the hard-switched energy by using 0.5 µF as C_{r2}, the energy of the FS-diode is increased under the same condition. To explain these results, Fig. 18 shows the waveforms of the hard-switched (shown with dotted lines) and soft-switched FS-diode. In this case, 0.5 µF is used as C_{r2}. The peak value of the reverse-recovery current is decreased by limiting di/dt with the auxiliary inductor, and dv/dt is also decreased by using C_{r2}. But this auxiliary circuit induces the long tail current and the large recovered charge (Q_{rr}). In the case of the SPT-diode, Q_{rr} at 0.5 µF is almost the same with Q_{rr} during the hard-switching. On the other hand, Q_{rr} at 0.5 µF is larger than Q_{rr} during the hard-switching in the case of the FS-diode. Besides, the trade-off relation of the forward voltage (V_F) and reverse-recovery energies (E_{rr}) are shown in Fig. 21. This V_F is measured at 600 A and 120 °C, and E_{rr} is measured at 600 A, 3.6 kV and 120 °C. Though the trade-off point of SPT-IGBT and FS-IGBT shown in Fig. 16 is almost equal, the point of SPT-diode and FS-diode is different. The diode with lower forward voltage (e.g. FS-diode) needs larger auxiliary capacitors, to reduce the reverse-recovery energy.

Fig. 19 shows the reverse-recovery energies and reduction rates of the diode with the blocking voltage of 3.3 kV. In this case, the reduction rate is slightly changed by increasing the auxiliary capacitors. The auxiliary inductor used in this measurement is large enough, and the influence of the auxiliary capacitor does not appear. The method to estimate the reverse-recovery energy with a certain auxiliary inductor from the measurements with one auxiliary inductor and several auxiliary capacitors has been already developed. Details of this method will be reported in future work.

Fig. 20 shows the reverse-recovery energies and reduction rates of the diode with the blocking voltage of 2.5 kV. In this case, the reduction rate is slightly changed by increasing the auxiliary capacitors from the same reason as the case of the 3.3 kV diodes.

The trade-off relation of the 3.3 kV diodes and the 2.5 kV diode shown in Fig. 21 shows the V_F and E_{rr} at 120 °C. V_F of 3.3 kV-diodes is measured at 1200 A, and the E_{rr} is measured at 1200 A and 1800 V. Furthermore, V_F of 2.5 kV-diodes is measured at 1200 A, and the E_{rr} is measured at 1200 A and 1250 V. These forward voltages are between the minimum and maximum voltages shown in the data sheets. The design point of the diode with 3.3 kV IEGT is almost equal to that of the diode with the 3.3 kV-NPT-IGBT (NPT-diode).

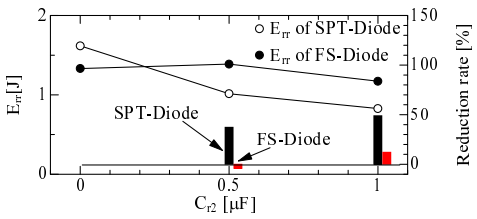

Fig. 17. Reverse-recovery energy of 6.5 kV diodes at 3600 V, 600 A and 120 °C

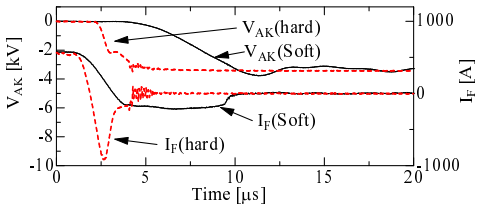

Fig. 18. Waveforms of the hard-switched and soft-switched 6.5 kV FS-Diode (C_{r1}, C_{r2}= 0.5 µF)

V. Conclusion

In this paper, the several high blocking voltage (above 2.5 kV) IGBTs on the market are evaluated under hard- and

Authorized licensed use limited to: Infineon Technologies AG. Downloaded on January 16,2023 at 08:48:59 UTC from IEEE Xplore. Restrictions apply.

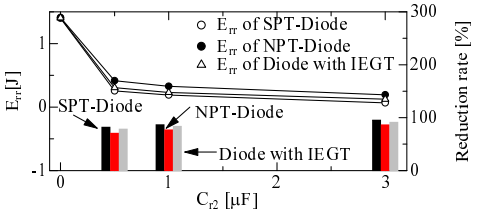

Fig. 19. Reverse-recovery energy of 3.3 kV diodes at 1800 V, 1200 A and 120 °C

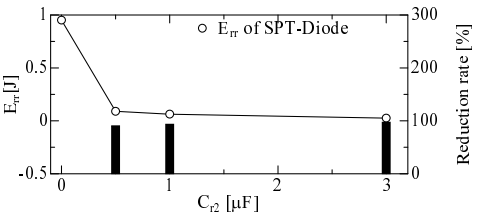

Fig. 20. Reverse-recovery energy of 2.5 kV diode at 1250 V, 1200 A and 120 °C

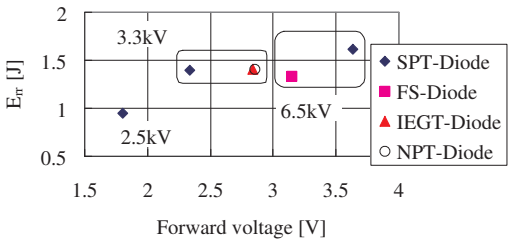

Fig. 21. Forward voltage and reverse-recovery energy of diodes at nominal voltage, current and 120°C

soft- switching conditions. To evaluate switching energy, the test bench, which can measure the switching energy of both hard-switched inverter and ARCPI, has been developed. This test bench consists of a step-up chopper circuit with three additional devices and is operated by means of a PC with LabVIEW. The control principle of the three devices is shown in this paper.

In the test bench, the voltage and current of the device under test are measured with an oscilloscope, which communicates with the PC via optical USB, and they are used to calculate the switching energy. The switching energy is interpolated with the function of the test voltage and current, in order to compare the switching energies with the nominal voltage and current.

From the results of turn-off energy measurements, it is clear that FS-IGBT and SPT-IGBT have similar characteristics. On the other hand, IEGT needs larger auxiliary capacitors than other IGBTs to achieve a similar reduction rate of the turn-off energy. That means devices with long carrier life time need larger auxiliary capacitors than devices with short carrier life time.

The measurements of the reverse-recovery energy show that the energy of FS-diode is not reduced by using 0.5 µF, because the recovery charge is increased by the small dv/dt caused of the auxiliary capacitors. Thus, it is important to reduce the recovery charge by choosing an appropriate auxiliary inductor.

ACKNOWLEDGMENT

We would like to thank Mr. E. Carroll of ABB Switzerland Ltd. for supplying the IGBTs to this project. In addition, we would like to thank Dr. R. Sommer of Siemens for supplying the IGBTs and the gate drivers.

REFERENCES

[1] F. Auerbach et al, "6.5 kV IGBT-modules", *Industry Applications Conference*, 1999, vol.3, pp. 1770 - 1774.

[2] J. G. Bauer et al, "6.5 kV-Modules using IGBT with Field Stop Technology", *International Symposium on Power Semiconductor Devices ICs*, 2001, pp. 121-124.

[3] T. Schuetze et al, "The New 6.5 kV IGBT Module: A Reliable Device for Medium Voltage Applications", *PCIM 2001*.

[4] M. Rahimo, et al, "Switching-self-clamping-mode "SSCM", a breakthrough in SOA performance for high voltage IGBTs and diodes", *The 16th International Symposium on Power Semiconductor Devices and ICs*, 2004, pp. 437 - 440.

[5] M. Rahimo et al, "Extending the Boundary Limits of High Voltage IGBTs and Diodes to above 8 kV", *International Symposium on Power Semiconductor Devices ICs*, 2002, pp. 41-44.

[6] T. Inoue et al, "New collector design concept for 4.5 kV injection enhanced gate transistor (IEGT)", *International Symposium on Power Semiconductor Devices ICs*, 2002, pp. 49-52.

[7] T. Ogura et al, "High turn-off current capability of parallel-connected 4.5 kV trench IEGT", in *IEEE Transactions of Electron Devices*, Vol. 50, Issue 5, May 2003, pp. 1392 - 1397.

[8] I. Omura et al, "Electrical and mechanical package design for 4.5 kV ultra high power IEGT with 6kA turn-off capability", *International Symposium on Power Semiconductor Devices ICs*, 2003, pp. 114 - 117.

[9] W. McMurray, "Resonant Snubbers With Auxiliary Switches", in Proceedings of *IAS Annual Meeting*, 1989, pp. 829 - 834.

[10] R. W. DeDoncker, J. P. Lyons, "The Auxiliary Resonant Commutated Pole Converter", in Proceedings of *IAS Annual Meeting*, 1990, pp. 1228 -1235.

[11] S. Bernet et al, "Evaluation of a high power ARCP voltage source inverter with IGCTs", in Proceedings of *IAS Annual Meeting*, 1999, vol.2, pp. 1063 - 1072.

[12] R. Teichmann et al, "State-of-the-art Low Voltage and High Voltage IGBTs in Soft Switching Operation", in Proceedings of *Applied Power Electronics Conference and Exposition*, 2003, vol.2, pp. 938 - 945.

[13] B. Gutsmann et al, "Repetitive Short Circuit Behaviour of Trench-/Field-Stop IGBTs", in Proceedings of *PCIM*, 2003.

[14] U. Schwarzer, R. W. De Doncker, R. Sommer, G. Zaiser, "Snubberless Operation of Series Connected 6.5 kV IGBTs for High-Power and High-Voltage Applications", in Proceeding of *EPE*, 2003.

Authorized licensed use limited to: Infineon Technologies AG. Downloaded on January 16,2023 at 08:48:59 UTC from IEEE Xplore. Restrictions apply.